Journal Pre-proof

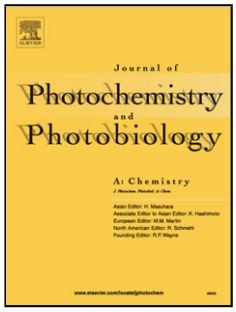

Design of novel anthracene-based fluorescence sensor for sensitive and selective determination of iron in real samples

Süreyya Oğuz Tümay, Mahsa Haddad Irani-nezhad, Alireza Khataee

PII: S1010-6030(20)30617-1

DOI: https://doi.org/10.1016/j.jphotochem.2020.112819

Reference: JPC 112819

To appear in: *Journal of Photochemistry & Photobiology, A: Chemistry*

Received Date: 18 June 2020

Revised Date: 21 July 2020

Accepted Date: 28 July 2020

Please cite this article as: { doi: https://doi.org/

Design of novel anthracene-based fluorescence sensor for sensitive and selective determination of iron in real samples

Süreyya Oğuz Tümay[a,1], Mahsa Haddad Irani-nezhad[b,2], Alireza Khataee[b,c,3*]

[a] Department of Chemistry, Gebze Technical University, 41400 Gebze, Turkey

[b] Research Laboratory of Advanced Water and Wastewater Treatment Processes, Department of Applied Chemistry, Faculty of Chemistry, University of Tabriz, 51666-16471 Tabriz, Iran

[c] Department of Environmental Engineering, Gebze Technical University, 41400 Gebze, Turkey

[*] Corresponding author:

a_khataee@tabrizu.ac.ir

Graphical abstract

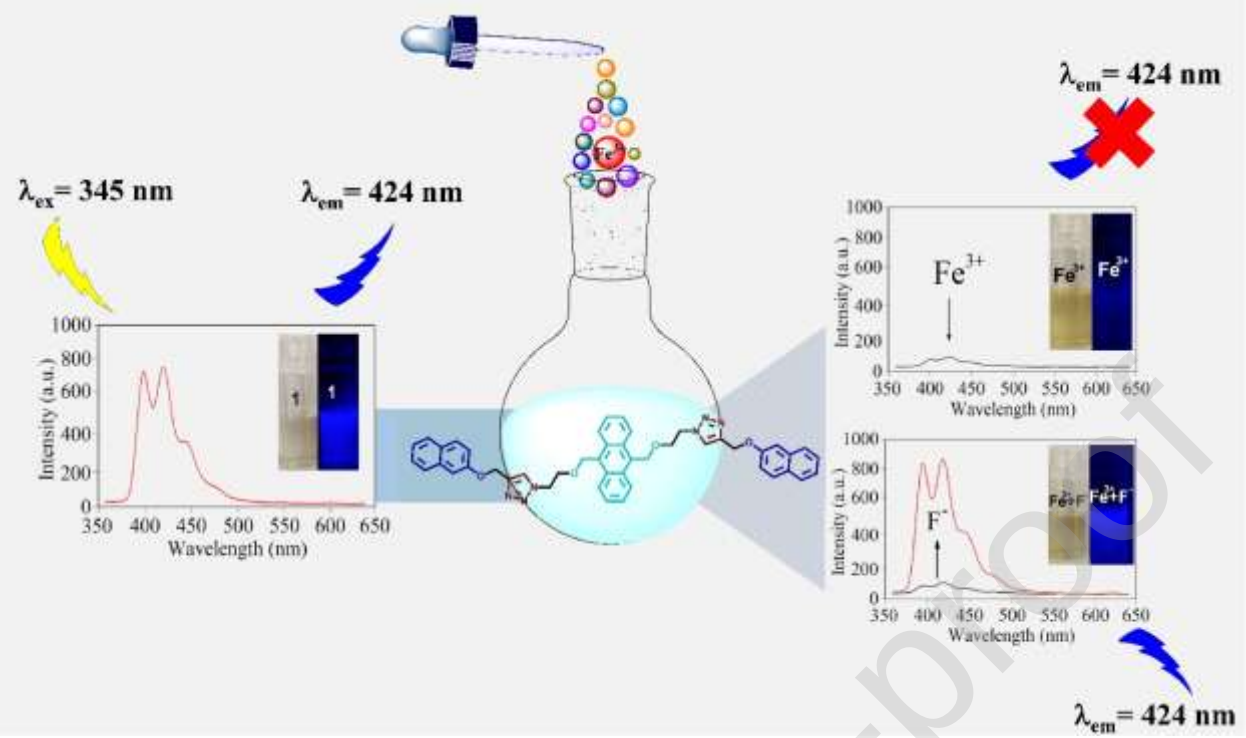

Research highlights

- Naphthalene appended dipodal anthracene sensor (**1**) was synthesized via a simple click reaction.
- Novel fluorescence sensor (**1**) demonstrated high sensitivity and selectivity towards Fe^{3+} over other competitive ions.
- The spectrofluorimetric determination of iron in environmental water and tablet samples was performed with using fluorescence sensor (**1**).
- The developed spectrofluorimetric method showed a good aggrement with ICP-OES analysis and spiked/recovery tests.

Abstract

A dipodal fluorescence (FL) system based on an anthracene platform was prepared by a general synthetic strategy. The water-miscible receptor was characterized by MALDI-MS, ^{1}H NMR, ^{13}C NMR, and FT-IR. In order to the illustration of photophysical properties of the synthesized sensor, the excitation–emission matrix (EEM) analysis and 3D-fluorescence measurements were performed. Ultraviolet-Visible (UV-Vis) and FL spectroscopies were carried out to evaluate the FL performance of the sensor. Low concentrations of iron ions (Fe^{3+}) could be determined by this sensitive and simple sensor. Due to the quenching effect of Fe^{3+}, a limit of detection (LOD) of 0.314 µM was obtained in the linear range of 0.3-130 µM. This fluorescent sensor was applied for measuring ferric ions in environmental water and tablet samples, which was highly efficient. The proposed strategy could be applied to develop sensors for not only for Fe^{3+} but also for many various metal ions using a diversity of fluorophores and ionophores.

Keywords: Dipodal receptor; Anthracene; Fluorescent sensor; Environmental water; Tablet.

1. Introduction

Fundamental roles in humans, plants, and animals are done by dissolved ions in aqueous media. Ions propagate the electronic signals and preserve the balance between intracellular and extracellular environments fluids that is very important for various processes such as muscle function, nerve impulses, regulation of pH level, and hydration [1]. The iron due to its important role in electron transfer, DNA, RNA (synthesis and repair), O_2 uptake, O_2 metabolism, and enzyme catalysis, is one of the most necessary paucity elements for life system [2]. Serious illnesses like Parkinson's and Alzheimer's diseases and cancers are caused by iron accumulation, while iron deficit leads breathing problems, diabetes, anemia, kidney, heart, and liver failure [3].

Although various instrumental methods have been applied in the iron detection including atomic absorption spectroscopy [4], ion pair chromatography [5], electrothermal atomization atomic absorption spectrometry (ETAAS) [6], voltammetry [7], and inductively coupled plasma mass spectrometry (ICP-MS) [8], in environmental, biological, and industrial samples, but they cannot be available in-field and achieved continuous monitoring. Also, they need pretreatment processes and some reagents like eluents and adsorbents [9]. These disadvantages have limited their applications. Therefore, the development of a determination method which solves the problems still is a challenge for researchers. Due to its easy operation, high sensitivity, rapid response, high efficiency, and remarkable selectivity, fluorescence (FL) is one of the most famous and appropriate approaches for the detection of iron in aqueous or organic media [10]. Fluoroionophore system is a part of fluorescent sensor systems which consists of the fluorophore and ionophore groups. The ionophore part interacts with metal ions while fluorophore moiety converts the diagnosis occurrence received from ionophore part to analytical signals [11]. Synthetic receptors provide wide range of properties in proportion of the targeted metal ions' shape

or size which is still a challenge for researchers to design new synthetic receptors with high selectivity. In target component detection by interaction/complexation of ion with receptor, synthetic receptor's topology has an especial role [12].

Until now, manifold fluorescent sensors have been reported for Fe^{3+} detection based on both fluorophore and ionophore systems however most of them because of low selectivity, high limit of detection (LOD), or narrow linear range are not so suitable. Kang and Kim [13] synthesized a chemosensor via the reaction of 2,3-dihydroxybenzaldehyde and octopamine for the detection of iron. This water-soluble and bio-friendly sensor has been used for detection of Cd^{2+} and Zn^{2+} by different FL emission (blue and green respectively). In another study, Gupta et al. [14] reported two fluorescence and colorimetric aminopyridine Schiff bases. They detected Fe^{3+}, UO_2^{2+}, Ni^{2+}, and Zn^{2+} via electrochemical, emission, and absorption properties of 2-((5-methylpyridin-2-ylimino)methyl)phenol and 1-((5-methylpyridin-2-ylimino)methyl)naphthalen-2-ol. Kim et al. [15] also developed a chemosensor for colorimetry detection of iron by changing the color from colorless to dark green. This benzimidazole-based sensor could be recycled by treating with ethylenediaminetetraacetic acid (EDTA).

Anthracene and its derivatives as fluorescent fluorophores, because of their easy process ability, unique properties, and commercial availability, have been applied in various functions such as sensing pH, small organic molecule, metal ions, and simple inorganic anions. Superior excimer and monomer emission variations occur via importing donor/acceptor units into anthracene backbones which is related to the space of two anthracene segments. So, tunable optical properties could be attained by controlling the shape/size of the materials [16]. Due to its low FL quantum yield [17] and short FL lifetime [18], naphthalene is of particular interest to be used as a donor or an acceptor [19].

Discerning different colures of weak light is the trait of human eye which eliminates using an expensive detector. These all results prompted us to prepare a novel fluorescent colorimetric sensor by "Click" reaction. So that, 1, 2, 3 triazole serves as a bridge between fluorophores (naphthalene and anthracene part) and acts as an ionophore to binds with analyte. The synthesized sensor (**1**) provides different FL colures when reacted with iron which can be recognized by the naked-eye upon UV light radiation. After the characterization of compound **1** via MALDI-MS, Nuclear magnetic resonance spectroscopy (^{1}H NMR and ^{13}C NMR), and Fourier transform infrared spectroscopy (FT-IR) methods, the excitation-emission matrix (EEM) analysis and 3D-FL measurements were carried out to illustration of its photophysical properties. Finally, compound **1** has been applied for the determination of Fe^{3+} in environments, industrial, and biological samples. Also, the validation of the sensor has been carried out via ICP-OES analysis and spike and recovery tests.

2. Experimental

2.1. Reagents

Tetrahydrofuran (THF), 2-naphthol, sodium hydride (NaH), copper(I) bromide, deuterated chloroform ($CDCl_3$), dimethyl sulfoxide (DMSO-d_6), N,N,N',N'',N''-pentamethyldiethylenetriamine (PMDTA), and N,N- dimethylformamide (DMF) were purchased from Sigma-Aldrich. Anthracene, *n*-hexane, paraformaldehyde, hexadecyltrimethylammonium bromide, sodium azide, dichloromethane, ethanol, glacial acetic acid, hydrogen bromide, acetonitrile (ACN), 2-bromoethanol were purchased from Merck and 2,5-dihydroxybenzoic acid which was used as MALDI matrix was obtained from Fluka. Washing with *n*-hexane was applied to purified NaH (>60%) because it is commercially available in mineral oil. Before using THF,

sodium/potassium alloy was used for distillation process. Inert argon or nitrogen atmosphere was used for all synthetic processes. Silica gel (70–230 mesh, Kieselgel 60) and silica gel plates/F_{254} (0.25 mm thickness, Kieselgel 60) were used for chromatography processes and they were purchased from Merck.

2.2. Equipments

The steady-state FL experiments and spectrofluorimetric analysis of real samples were performed by Cary Eclipse spectrofluorometer (Varian, USA). Fluorolog 3-2iHR with Fluoro Hub-B Single Photon Counting Controller (Horiba Jobin Yvon, France) was used for time resolved-FL, 3D-FL emission experiments and excitation-emission matrix analysis. Recording of FL emission signal for time resolved-FL, 3D-FL measurements and excitation-emission matrix analysis was performed by TCSPC module. Slit widths were selected 5 nm and pathlength was 1 cm for all experiments and they were performed at 25^{o}C. 2101-UV spectrophotometer (Shimadzu, Japan) and INOVA 500 MHz spectrometer (Varian, USA) used for UV-Vis absorption and NMR (^{1}H and ^{13}C) experiments. MALDI-TOF mass spectrometer (Bruker Daltonics Microflex, USA) and Spectrum 100 spectrophotometer (Perkin Elmer, USA)were used for recording of mass and FT-IR spectra of novel compounds. Non-linear regression analyses were applied by equations using Sigma-Plot 14.0.

2.3. Synthesis of compounds

Synthesis and purification of 2-azido-1-ethanol, 9,10-bis(bromomethyl)anthracene, 2-(prop-2-yn-1-yloxy)naphthalene were performed according to the literature [20]. **N_3-L** and **1** which were newly synthesized compounds were characterized by ^{1}H, ^{13}C NMR, FT-IR and MALDI-MS

spectra spectroscopies. All characterization results were consistent with structures of compounds and they were given in Fig S1-S4.

2.3.1. 9,10-bis((2-azidoethoxy)methyl)anthracene (N_3-L)

2-azido-1-ethanol (1.196 g, 13.73 mmol) and NaH (0.549 g, 13.73 mmol) was added in THF (50 mL) under inert atmosphere and obtained suspension was refluxed for 30 min. After, 9,10-bis(bromomethyl)anthracene (2.000 g, 5.490 mmol) which dissolved in THF (50 mL) was added dropwise to suspension and reaction mixture was refluxed for 24 h. The reaction was followed by TLC (silica gel used as stationary and 5 *n*-hexane: 1 ethylacetate (v/v) used as an eluent). After reaction finished, G4 filter was used for filtration of reaction mixture and the organic solvent of mixture was removed with using rotary evaporator under reduced pressure. Crude product was purified by column chromatography (silica gel used as stationary and 5 *n*-hexane: 1 ethylacetate (v/v) used as an eluent) and **N_3-L** was obtained as light yellow solid (1.650 g, 80%, m.p. 92^{o}C). ^{1}H NMR (δ_{ppm}, 298 K, DMSO-d_6); 8.50 (dd, J = 6.9, 3.1 Hz, 2H), 7.61 (dd, J = 6.9, 3.1 Hz, 2H), 5.53 (s, 2H), 3.86 (t, J = 4.8, 2H), 3.47 (t, J = 4.8, 2H). ^{13}C NMR (δ_{ppm}, 298 K, DMSO-d_6); 130.25, 130.01, 125.80, 124.10, 68.76, 64.30, 50.10. FT-IR (ATR, cm $^{-1}$); 3094-3024 (-C=H), 2981– 2860 (-C-H), 2086.6 (-N=N=N), 1850-1650 (-C=C-), 1350-1250 (-C-H-). $[M+H]^+$: 377.272 m/z (calc. $[M+H]^+$: 377.420).

2.3.2. 9,10-bis((2-(4-((naphthalen-2-yloxy)methyl)-1H-1,2,3-triazol-1-yl)ethoxy)methyl) anthracene (1)

N_3-L (0.200 g, 0.531 mmol), Cu(I)Br (0.229 g, 1.593 mmol), PMDTA (0.276 g, 1.593 mmol) and 2-(prop-2-yn-1-yloxy)naphthalene (0.242 g, 1.328 mmol) were dissolved in dry

dichlorometane (10 mL) under inert atmosphere. The obtained solution was stirred at room temperature for 24 h and followed by TLC (silica gel used as stationary and 2 THF: 1 *n*-hexane (v/v) used as an eluent). After completion of the reaction, it was extracted with dichloromethane/H_2O. The organic phase was dried over Na_2SO_4 and rotary evaporator was used to remove organic solvent. Crude product was purified by column chromatography (silica gel used as stationary and 2 THF: 1 *n*-hexane (v/v) used as an eluent). Compund **1** was obtained as white/light yellow solid (0.268 g, 68%, m.p. 186^{o}C). ^{1}H NMR (δ_{ppm}, 298 K, $CDCl_3$); 8.25 (dd, *J* = 6.6, 3.1 Hz, 4H), 7.73 (dt, *J* = 16.1, 7.7 Hz, 8H), 7.49 (dd, *J* = 6.7, 3.1 Hz, 4H), 7.43 (t, *J* = 7.4 Hz, 2H), 7.34 (t, *J* = 7.4 Hz, 2H), 7.21 (s, 2H), 7.11 (d, *J* = 10.2 Hz, 2H), 5.48 (s, 4H), 5.18 (s, 4H), 4.53 (t, *J* = 4.3 Hz, 4H), 4.04 (t, *J* = 4.3 Hz, 4H). ^{13}C NMR (δ_{ppm}, 298 K, $CDCl_3$); 156.24, 134.39, 130.58, 129.63, 129.11, 127.64, 126.88, 126.42, 126.10, 124.60, 123.84, 118.82, 107.18, 68.58, 64.40, 61.91, 37.48. FT-IR (ATR, cm $^{-1}$); 3074-3028 (-C=H), 2980– 2863 (-C-H), 1850-1650 (-C=C-), 1350-1250 (-C-H-). $[M]^+$: 740.901 m/z and $[M+Na+K]^+$: 802.042 (calc. $[M]^+$: 740.86 and $[M+Na+K]^+$: 802.86).

2.4. Real samples

Environmental water samples and medicine tablets were collected from Istanbul/Kocaeli, Turkey. After filtration process of the samples by blue band filter paper, HNO_3 (70%) was used for the acidification of all samples. Before using for real sample analysis they stored at 4 ^{o}C in the refrigerator. Medicine tablet samples were prepared for analysis according to the previous report [21].

2.5. Measurement procedure

Sensitive and selective complexation of the presented FL sensor (**1**) with iron allowed spectrofluorimetric analysis of iron level in real samples without any enrichment processes. The FL emission of **1** in blue region which were originated from anthracene moiety significantly quenched after complexation of **1** with iron. Because of HNO_3 (70%) and other acidic medium of digested and stored processes of real samples, Fe^{2+} ions of medicine tablets and environmental water samples were oxidized to Fe^{3+}. Therefore, complexation of **1** with Fe^{3+} was basis of presented spectrofluorimetric determination method of iron. The determination of iron amount of real samples was performed by calibration curve which was obtained with various amount of Fe^{3+} of water samples. Equation (1) was used for calculation of iron quantity.

$$C_{Fe^{3+}} = \frac{[(F_0 - F)/F_0] - n}{m} \qquad (1)$$

where *m*, *n*, *F* and F_0 are the slope of the calibration curve, intercept of FL emission signal axis, FL emission signal of **1**+Fe^{3+} and FL emission signal of **1** in the absence of Fe^{3+} (1:1 v/v, pH 8.0, λ_{ex}=345 nm, 2 μM **1**), respectively. In addition, $(F_0\text{-}F)/F_0$ and C_{Fe}^{3+} are relative FL signal of **1**+Fe^{3+} and iron concentration of real samples, respectively. The emission of anthracene moiety which was the origin of the FL emission of sensor **1** was quenched with increased concentration of Fe^{3+}. This FL quenching was gradual and proportional until 130 μM of Fe^{3+} and it was applicable for determination of iron real sample. Spectrofluorimetric analysis of iron with FL sensor **1** in medicine tablets and environmental water samples was performed as follows; $5x10^{-4}$ M of **1** was prepared in DMSO and it was used as stock solution. 0.200 mL of **1** was taken from stock solution and added to 10 mL volumetric flask with 4.8 mL of DMSO. After, Britton–Robinson (B-R, 0.5

mL, pH 8.0) and real samples (0.5 mL) added to flask, the volume of flask was completed to 10 mL with deionized water. Finally, obtain solution was shaken carefully for 10 seconds. The spectrofluorimetric analysis was performed according to relative FL response of **1**+Fe^{3+} complex which was recorded at 424 nm after optimization studies. The accuracy of the developed spectrofluorimetric determination method was investigated by spike/recovery measurements and inductively coupled plasma-optical emission spectrometry (ICP-OES) analysis under optimum analytical conditions.

2.6. Photophysical properties

The comparative method (Eq. (2)) was used for the calculation of the FL quantum yields (ΦF) of **1** and **1**+Fe^{3+} complex [22].

$$\emptyset F = \emptyset F_{Std} \frac{F.A_{Std}.n^2}{F_{Std}.A.n_{Std}^2} \qquad (2)$$

where *n*, *F*, F_{Std}, *A*, and A_{Std} are the refractive indices of solvents which were used for dissolution of **1** and standard, FL peaks areas of FL sensor and standard, absorbance bands areas of FL sensor and standard at same analytical conditions. In this study, we used quinine sulfate which has ΦF = 0.54 in 0.1 M H_2SO_4 as a standard [23].

The FL lifetimes of **1** and **1**+Fe^{3+} complex was directly measured by time-correlated single-photon counting (TCSPC) method with appropriate exponential calculations. All lifetime measurements were performed with nanoLED (Horiba Jobin Yvon, France) at 390 nm as a light source. The excitation–emission matrix (EEM) analysis and 3D-FL measurements were obtained by CCD detector on Fluorolog 3-2iHR (Horiba Jobin Yvon, France) .

3. Results and discussion

3.1. Synthesis/structural characterization

Click chemistry has been extensively applied for metal determination studies with FL sensors. Because 1,2,3 triazoles which are obtained as a result of Cu(I)-catalysed azide–alkyne cycloaddition reaction can serve not only a bridge between ionophore and fluorophore groups but also it can be used as ionophore [24]. Up to now, some fluorescent sensors for different metal ions such as Pb^{2+}, Ni^{2+}, Cd^{2+}, Zn^{2+}, Ag^{+}, Hg^{2+} and Fe^{2+}/Fe^{3+} were synthesized via click chemistry to form triazole groups as metal ions binding site, which were consisted from different alkoxy chain lengths and chemical structures [9,24-27]. Apart from the chemical structure, alkoxy chain lengths of triazole binding sites affect the sensitivity and selectivity of fluorescent sensors towards metal ions which could be optimized via alkoxy chain lengths [24-26]. In recent years, due to its important role in biological processes and industry, there are many fluorescent sensors that existed in literature based on click chemistry and selective for iron [9,24,27]. With the experience that we have gained from literature about chemical structures of click chemistry-based iron selective fluorescent sensors, in this study, we synthesized di-podal anthracene-based FL sensor with click reaction for spectrofluorimetric analysis of iron in real samples. For that purpose, synthesis and characterization of 2-azido-1-ethanol, 9,10-bis(bromomethyl)anthracene, 2-(prop-2-yn-1-yloxy)naphthalene were performed via reported procedures of the literature [20]. Then, as a result of nucleophilic substitution reaction of 2-azido-1-ethanol and 9,10-bis(bromomethyl)anthracene in the presence of NaH, **N_3-L** which was azide-functionalized core compound was obtained. Finally, di-podal anthracene-based FL sensor (**1**) was obtained by click reaction of **N_3-L** with 2-(prop-2-yn-1-yloxy)naphthalene (68% yield) (Scheme 1). Column chromatography was applied to purify all novel compounds and MALDI-MS, ^{1}H, ^{13}C NMR and FT-IR spectroscopies were used

for chemical characterization of **N_3-L** and **1** (Fig S1-S4). In this work, triazole groups are designed as ionophores while naphthalene/anthracene groups are designed as fluorophore groups that convert recognition into analytical signals.

Scheme 1.

As can be seen from ^{1}H NMR spectra of **N_3-L** and **1** (Fig S2 (a and b)), symmetric aromatic anthracene peaks are observed in **N_3-L** at 8.50 ppm and 7.61 ppm while at compound **1**, triazole and aromatic naphthalene peaks were observed with aromatic anthracene peaks between 8.26-7.10 ppm. In addition, integration values and chemical shifts of aromatic and methylene proton in the ^{1}H NMR spectra of **N_3-L** and **1** compatible with their structures.

According to FT-IR spectra of **N_3-L** and **1** (Fig S4), H-C≡C- stretching vibrations of 2-(prop-2-yn-1-yloxy)naphthalene observed at 3293 cm^{-1}. In addition, obtained -N=N=N (azide) vibration which was observed at 2086 cm^{-1} after nucleophilic substitution reaction of 2-azido-1-ethanol with 9,10-bis(bromomethyl)anthracene confirmed chemical structure of **N_3-L** in the FT-IR spectrum. After click reaction of **N_3-L** with 2-(prop-2-yn-1-yloxy)naphthalene to obtain FL sensor **1**, H-C≡C- stretching vibrations of 2-(prop-2-yn-1-yloxy)naphthalene and N=N=N (azide) vibration of **N_3-L** were disappeared. -CH and -C=H vibrations existed in FT-IR spectrum which supported the formation of FL sensor **1** (Fig S4).

3.2. Spectroscopic studies of compound 1

The absorption and FL properties of **1** were studied in various solvents including *n*-hexane, THF, dichloromethane, ACN, ethanol, DMF, DMSO, water, and DMSO: water (1:1) with different concentrations via Ultraviolet-Visible (UV-Vis) absorption and FL spectrophotometer at 25 °C.

According to Fig. S5, absorption properties of **1** do not differ by changing the solvent system and compound **1** insoluble in *n*-hexane. The difference in the absorbance intensity is probably related to the difference in the dissolution of compound **1** in various solvents. Since compound **1** contains both naphthalene and anthracene parts, its UV-Vis spectrum has two electronic absorption maxima which are located at wavelengths of 274 nm and 366 nm and they are ascribed to π–π* transition [24]. Also, the same solvents were used to investigate the FL emission of **1**. According to the Fig S6, severe FL emission responses are perceived at about 410 nm and 424 nm (λ_{ex}= 345 nm) for prepared compound **1** (except in water), which is consistent with reported results for FL emission of anthracene. According to the results of Fig S5 and S6, the solvents systems do not affect so the optical properties of **1**, except in more polar solvents such as water the excimer emission vanishes which is related to the π- stacking interactions disrupting [9]. Aqueous DMSO system (1:1 v/v) gives suitable FL signals at 410 nm and 424 nm with a 50 nm Stokes shift for spectrofluorimetric detection of Fe^{3+} in environmental water samples (Fig S7).

3.3. Optimization of compound 1 procedures

In order to get high sensitivity and selectivity of the compound **1** complexation procedure for Fe^{3+} detection, the reaction conditions were optimized. The effects of the influential parameters including competitive ions, initial **1** concentration, pH, time before measurement, and buffer concentration were investigated.

3.3.1. Effect of competitive metal ions

The most important parameter in FL sensors is its selectivity which becomes even more significant for analysis of real samples. UV-Vis absorption and FL spectroscopies were used for

studying the selectivity of **1**. All spectral determinations were carried out in spectroscopic quartz cuvette with final solution volume of 10 mL via applying micropipette at room temperature. The stock solutions of chloride salts of cations (except for Pb^{2+} and Ag^{+}) were prepared in water whilst the stock solution of **1** was prepared in DMSO. UV-Vis and FL characteristics of compound **1** in buffered aqueous DMSO solution (1:1 v/v and pH 8.0) were evaluated by addition of 130 µM various competitive metal ions like Fe^{3+}, Fe^{2+}, Zn^{2+}, Pb^{2+}, Ni^{2+}, Na^{+}, Mn^{2+}, Mg^{2+}, Li^{+}, Hg^{2+}, K^{+}, Cu^{2+}, Cd^{2+}, Ca^{2+}, Cs^{+}, Co^{2+}, Cr^{2+}, Ba^{2+}, Al^{3+}, and Ag^{+} when excited at 345 nm. According to Fig 1a, addition of Fe^{2+}/Fe^{3+} to 10 µM sensor **1** causes significantly increase (about 4 fold) in UV-Vis absorption whereas other different metal ions addition does not affect absorption spectra. These increases in UV-Vis absorption spectra of compound **1** attributed to the formation of compound **1**-$Fe^{3+/2+}$ complexes, which causes the electron reorganization with adding of $Fe^{3+/2+}$ [28]. Also, significant color change is observed by adding Fe^{3+}/Fe^{2+} to aqueous DMSO solution of **1** while other different metal cations don't make remarkable changes in solution color at daylight (Fig 1c). In order to investigate the selectivity of the sensor, the FL of 2 µM compound **1** was also evaluated in the presence of competitive metal cations with the identical operation conditions with UV-Vis electronic absorption spectroscopy. As it can be observed at Fig 1b and 1d, by adding Fe^{3+}/Fe^{2+} to the sensor **1**, its FL emission signal is fully quenched, along with FL colure change from colorless to yellow. The FL quenching is generally explained via chelation enhanced fluorescent quenching (CHEQ) mechanism in which coordination of paramagnetic guests like Fe^{3+} and Fe^{2+} with the host causes the quenching of the fluorophore FL emission [29].

Fig 1.

As shown at Fig 2, the relative FL intensity changes of compound **1** in the presence of cations (Fe^{3+}, Fe^{2+}, Zn^{2+}, Pb^{2+}, Ni^{2+}, Na^{+}, Mn^{2+}, Mg^{2+}, Li^{+}, Hg^{2+}, K^{+}, Cu^{2+}, Cd^{2+}, Ca^{2+}, Cs^{+}, Co^{2+}, Cr^{2+}, Ba^{2+}, Al^{3+}, and Ag^{+}), anions (SO_4^{2-}, CN^{-}, F^{-}, I^{-}, $H_2PO_4^{-}$, HSO_4^{-}, NO_3^{-}, CO_3^{2-}, Cl^{-}, $S_2O_3^{-}$, NO_2^{-}, S^{2-}, CH_3COO^{-}, SCN^{-}) and single molecules (ascorbic acid, catechin, rutin, quercetin, citric acid, caffeic acid and oleic acid) confirms the selectivity of the sensor towards Fe^{3+}/Fe^{2+} detection. The difference of proposed sensor **1** relative FL intensity between iron-free metal blend and iron-containing metal blend demonstrates that different competitive ions do not affect the relative FL intensity of **1**.

Fig 2.

3.3.2. Effect of pH

Due to the efficacy of pH on the chemical structure of **1** and its complexation with Fe^{3+}, pH of the solution is one of the main parameters for quantitative recovery. Therefore, the effect of various pH values (4.0-10.0) with Britton-Robinson (B-R) buffer system on relative FL responses of **1**+Fe^{3+} was examined while other operational conditions were kept constant. Maximum relative FL emission intensity is observed at pH 8.0 and it decreases below and above 8.0 (Fig S8a). Above pH 6, compound **1** acts mainly as an electron donor, thus relative FL emission signal increases significantly [30]. Since the formation of complex, sensitivity, and selectivity were considered, Britton-Robinson buffer with pH 8.0 was selected for determination process of environmental water samples.

3.3.3. Effect of the B-R buffer concentration

Determination of appropriate buffer with proposed medium pH is needed to attain stable Fe^{3+}-compound **1** complexes [30]. Therefore, the evaluation of efficacy of the B-R buffer solution's quantity on the interaction of **1** with Fe^{3+} should be performed. In order to this purpose, the effect of B-R buffer solutions with different concentrations from 0.1 M to 0.4 M on relative FL emission signal of the complex was studied. As demonstrated in Fig S8b, by increasing the concentration of the B-R buffer above 0.1 M, the relative FL intensity of Fe^{3+}- compound **1** decreases. So, 0.1 M B-R buffer solution is suitable for complexation process.

3.3.4. Effect of initial 1 concentration

Initial **1** concentration is another parameter which should be optimized to get more sensitivity. For this aim, different concentrations of **1** ranging from 1 µM to 4 µM were prepared in aqueous DMSO solution (1:1 v/v). The differences in the intensity of relative FL by adding Fe^{3+} have been investigated in Fig S8c. When **1** concentration changes from 1 µM to 2 µM, the relative FL intensity increases. But by following the concentration increasing up to 4 µM, the intensity of relative FL decreases sharply. This behavior could be attributed to intermolecular self-quenching of anthracene groups in high concentrations that have been observed for several fluorophores [31]. According to obtained results, 2 µM was chosen as sufficient **1** concentration for the Fe^{3+} detection process in real samples.

3.3.5. Effect of measurement time

The time before determination is a parameter that affects the complexation of **1** with Fe^{3+}. So, its effect on Fe^{3+} detection process was evaluated in the range of 0-50 second (s) while other

parameters kept constant. As illustrated in Fig S8d, when 2 μM of **1** in buffered aqueous DMSO solution (1:1 v/v, pH 8.0) is used, the maximum intensity of relative FL is obtained at 10 s and then increasing the time doesn't show any effect on FL intensity. Therefore, the determination process carried out after 10 s in real samples, considering the stability of **1**+Fe^{3+} complexes.

3.4. Formation of 1-Fe^{3+} complexes and quenching mechanism of 1 by Fe^{3+}

In order to study the formation of **1**- Fe^{3+} complexes, Job's (continuous variation) plot and also non-linear curve fitting analyses were carried out in water:DMSO (1:1 v/v, pH 8.0) [32]. Job's (continuous variation) plot was obtained by using 2 μM compound **1** and Fe^{3+} ions mole fraction increasing in complexes (Fig S9a). The maximum FL intensity of complexes attains at 0.5, it can be concluded that **1**+Fe^{3+} complexes stoichiometry is 1:1 (metal:ligand). As can be observed at non-linear curve fitting analysis (Fig S9b), by addition of Fe^{3+} to compound **1**, relative FL intensity increases and an inflection point is demonstrated at plot where 1:1 (metal:ligand) stoichiometry was determined for compound **1** to Fe^{3+}. The results obtained from non-linear curve fitting plots and Job's plot analysis are in compatibility with each other.

In FL sensor applications, the photostability of receptors and complexes is necessary to obtain highly accurate and precise results. 2 μM compound **1** containing 130 μM Fe^{3+} in buffered aqueous DMSO solution (1:1 v/v, pH 8.0) was used to appraise photostability of **1**. Then, the FL measurements were performed between 0 and 60 minutes in daylight. As can be seen at Fig S10, compound **1** and its complex with Fe^{3+} both are highly photostable and their relative FL intensities are unaffected and relatively constant during 60 min. In order to appraise the reversibility of the compound **1** reversibility towards Fe^{3+}, fluoride ions (F^-) were added to Fe^{3+}-**1** complexes. Restitution of the increased UV-Vis absorption and quenched FL intensity of compound **1** by

adding Fe^{3+} after addition of different concentrations of F^- demonstrates that identification of Fe^{3+} is a complexing and reversible process (Fig 3 (a-d)).

Fig 3.

FL quenching process occurs in two different ways: dynamic and static processes. Static quenching is caused by nonfluorescent complex, when a quencher and fluorophore complexes in ground state. Encounter of quencher and excited state of fluorophore molecules causes dynamic quenching process [33]. So, FL lifetime of the fluorophore is imported in dynamic process which must be reduced while it does not affect the static process. The FL emission intensity is also affected by the quencher concentration which can shed light into the quenching mechanism. A quencher's performance in the quenching mechanisms is given by Stern-Volmer equation (Eq. (3)) [34]:

$$I0/I = Ksv[Q]+1 \qquad (3)$$

where, I_0, I, K_{sv}, and Q represent the initial FL intensity of a fluorophore (**1**), final FL signal of a fluorophore in the quencher presence (Fe^{3+}), Stern-Volmer constant, and quencher's concentration (molar). According to Stern-Volmer relationship, in static quenching a linear graph obtains from plotting of I_0/I against [Q] with y-axis intercept of 1. Positive deviation observation in the graph by increasing quencher concentration demonstrates that the effective quenching mechanisms in the system are both dynamic and static quenching [24]. Stern-Volmer plot of Fe^{3+}-**1** complex is demonstrated at Fig S11a. As the results show, by increasing Fe^{3+} concentration until 9×10^{-5} M,

the I_0/I increase linearly and further the positive deviations are perceived for Fe^{3+}-**1**. So, it can be understood that FL intensity quenching process of compound **1** is included both dynamic and static quenching. As pointed before, an alternative way to recognize quenching process is FL lifetimes. So, the FL lifetime determinations of compound **1** and in the presence of Fe^{3+} and F^- were carried out (Fig S11b). The FL lifetimes were calculated as 9.135±0.012 ns (τ_0), 8.867±0.015 ns (τ_1), 8.951±0.017 ns (τ_2) for compound **1**, compound **1**+Fe^{3+}, and compound **1**+Fe^{3+}+F^-, respectively. Owing to the formation of Fe^{3+}-**1** complex in ground state, slight differences might be seen in the FL lifetimes of free sensor and complex. When the Fe^{3+}-**1** complex forms, sensor **1** becomes non-fluorescent and in the FL lifetime determination, the static quenching causes deletion of this non-fluorescent part. Therefore, the FL lifetime is due to non-complexed compound **1** and the FL properties of free part of compound **1** remain initial. So, it is expected that in static quenching process τ_0/τ to be ~1 [33,9]. The rate of the FL lifetimes of **1** (τ_0) and its complex with Fe^{3+} (τ) was calculated as 1.03. According to results, it seems that the effective mechanism for **1**+Fe^{3+} complexation is static quenching.

3.5. Analytical figures of sensor 1

FL titration experiments were performed by 2 µM of compound **1** and different concentrations of Fe^{3+} (0-130 µM) and F^- (0-450 µM) with the aim of determination of dynamic range of the sensor. As shown at Fig 3c and 3d, when Fe^{3+} concentration increases gradually, relative FL emission intensity proportionally quenches at 424 nm and by adding F^- to the sensor, the FL intensity increases again. Fig 4 demonstrates the calibration curves of **1**-Fe^{3+} and **1**-Fe^{3+}+F^-. According to the calibration curves, the linear ranges of the sensor are between 0.3-130 µM of Fe^{3+} ($(F_0-F)/F_0 = 0.0068C_{Fe^{3+}} + 0.054$, R^2=0.9973) and 0.3-450 µM of F^- ($(F_0-F)/F_0 = -0.002C_{F^-}$ +

0.9683, R^2=0.9945) with limit of detection (LOD) of 0.314 µM, which is calculated with using 3σ/k (where k: the calibration curve's slope, σ: the blank solution's deviation). The limit of quantification (LOQ) was also computed as 0.942 µM for Fe^{3+} detection. Importantly, obtained LOD and LOQ values for determination of Fe^{3+} with presented spectrofluorimetric method is lower than the maximum EPA's permitted level of Fe^{3+} ions in drinking water (5.4 µM or 0.3 ppm) [35]. Another important parameter for consistent results is precision. Under optimized conditions, the calculated relative standard deviation (RSD%) for Fe^{3+} was 2.89% (N=10). Table S1 displays the analytical performance of **1,** which the high sensitivity, selectivity, and reproductively of the sensor can be concluded.

Fig 4.

3.6. Compound 1 excitation–emission matrices (EEMs) changes during Fe^{3+} detection process

Comparative content of the fluorescent components is the information obtained from EEM spectra [36]. Target analytes' composition is provided from peak position and their red or blue shifts is related to their surroundings and sources [37]. Unlike UV-Vis, intrinsic FL is comprising data about dynamic properties due to intermolecular and intramolecular interactions, as well as substances' heterogeneity, conformation, structure, and functional groups [38]. According to Fig 5, compound **1** is a fluorescent substance and the presence of Fe^{3+} and F^- is effective on its FL spectra. **1** has an emission peak which is located at 400-500 nm and indicates its blue emission (Fig 5a, S12a). On the other hand, addition of Fe^{3+} quenches the FL intensity of **1**, which illustrates

the interaction of Fe^{3+} with compound **1** (Fig 5b, S12b). Further, when F^- is augmented **1**+Fe^{3+} complex separates and FL intensity of **1** restore (Fig 5c, S12c).

Fig 5.

3.7. Analysis of real samples

The performance of the method for analysis of real samples through Fe^{3+} measurement was appraised in environmental water samples and medicine tablets. For this purpose, spike and recovery tests and also official ICP-OES method were performed. Environmental water and medicine tablet samples were spiked between 0 and 75 µM Fe^{3+} and the purposed FL method was exerted under optimum conditions. As demonstrated in Table 1, the obtained quantitative recoveries with low RSD% are in good agreement with spiked amounts of analyte. ICP-OES was used as an official method in order to more verification of the pointed FL method accuracy (Table 2) and the evaluation of the differences between 2 methods was carried out by the Student t-test, which the results can be seen at Table S2. According to the results, the differences were found to be insignificant. The obtained results including RSD%, recoveries, and t-test demonstrate the high precision and accuracy of the presented FL method for the determination of Fe^{3+} in tablet and water samples. The presented FL method was compared with some other analytical methods such as potentiometry, spectrophotometry and spectrofluorimetry for determination of iron content of real samples and results were given at Table S3. According to Table S3, presented FL method has higher sensitivity, wider linear range and importantly lower limit of detection than given potentiometric, spectrophotometric and spectrofluorimetric methods, without interfering [S1-9]. The simple and efficient spectrofluorimetric determination of iron in real samples can performed

at natural pH in several seconds due to sensitive and selective interaction of **1** with iron. Although some determination methods which based on spectrophotometry has lower detection limit than presented method, enhancement procedures using eluent and adsorbent are applied before determination via these methods [S10]. The results of comparison revealed that, presented spectrofluorimetric method is simple, selective, time-efficient, accessible and sensitive determination method for iron in real samples.

Table 1

Table 2

4. Conclusion

A novel dipodal receptor based on anthracene was introduced with the quenching effect of iron ions, which could be used as a sensor for Fe^{3+} detection. The synthesis of this turn-off fluorescent sensor was performed by the proposed synthetic strategy. FL spectroscopy and UV–Vis absorption demonstrated the sensor's high sensitivity and selectivity towards iron ions at low levels. ICP-OES analysis, spike and recovery tests were carried out to validate the introduced sensor, which showed the high accuracy of the sensor. This approach with LOD of 0.314 µM in the linear range of 0.3-130 µM could be appropriate for spectrofluorimetric analysis in biological and water samples for quantification of iron level. More importantly, the proposed strategy could be used for obtaining novel sensors for many various metal ions using a diversity of fluorophores and ionophores.

Author contributions

Alireza Khataee acted as a supervisor. Material preparation, data collection and analysis were performed by Süreyya Oğuz Tümay. The first draft of the manuscript was written by Mahsa Haddad Irani-nezhad and all authors commented on previous versions of the manuscript. All authors read and approved the final manuscript.

Electronic supplementary material

The online version of this article contains supplementary material, which is available to authorized users.

Declaration of interests

The authors declare that they have no known competing financial interests or personal relationships that could have appeared to influence the work reported in this paper.

Acknowledgments

We thank Gebze Technical University and University of Tabriz for the support provided.

References

1. Ghittorelli M, Lingstedt L, Romele P, Crăciun NI, Kovács-Vajna ZM, Blom PW, Torricelli F (2018) High-sensitivity ion detection at low voltages with current-driven organic electrochemical transistors. Nature communications 9 (1):1-10

2. Guo L, Tang T, Hu L, Yang M, Chen X (2017) Fluorescence assay of Fe (III) in human serum samples based on pH dependent silver nanoclusters. Sensors and Actuators B: Chemical 241:773-778

3. Şenol AM, Onganer Y, Meral K (2017) An unusual "off-on" fluorescence sensor for iron (III) detection based on fluorescein–reduced graphene oxide functionalized with polyethyleneimine. Sensors and Actuators B: Chemical 239:343-351

4. Grotti M, Abelmoschi ML, Soggia F, Frache R (2003) Determination of ultratrace elements in natural waters by solid-phase extraction and atomic spectrometry methods. Analytical and bioanalytical chemistry 375 (2):242-247

5. García-Marco S, Torreblanca A, Lucena JJ (2006) Chromatographic determination of Fe chelated by Ethylenediamine-N-(o-hydroxyphenylacetic)-N'-(p-hydroxyphenylacetic) acid in commercial EDDHA/Fe^{3+} fertilizers. Journal of agricultural and food chemistry 54 (4):1380-1386

6. Prkić A, Mitar I, Giljanović J, Sokol V, Bošković P, Dolanc I, Vukušić T (2018) Comparison of potentiometric and ETAAS determination of copper and iron in herbal samples. International Journal of Electrochemical Science 13:9551-9560

7. Bobrowski A, Nowak K, Zarębski J (2005) Application of a bismuth film electrode to the voltammetric determination of trace iron using a Fe(III)–TEA–BrO_3^- catalytic system. Analytical and bioanalytical chemistry 382 (7):1691-1697

8. Konz T, Añón Alvarez E, Montes-Bayon M, Sanz-Medel A (2013) Antibody labeling and elemental mass spectrometry (inductively coupled plasma-mass spectrometry) using isotope dilution for highly sensitive ferritin determination and iron-ferritin ratio measurements. Analytical chemistry 85 (17):8334-8340

9. Tümay SO, Sarıkaya SY, Yeşilot S (2018) Novel iron (III) selective fluorescent probe based on synergistic effect of pyrene-triazole units on a cyclotriphosphazene scaffold and its utility in real samples. Journal of Luminescence 196:126-135

10. Jalili R, Khataee A (2019) Aluminum (III) triggered aggregation-induced emission of glutathione-capped copper nanoclusters as a fluorescent probe for creatinine. Microchimica Acta 186 (1):29

11. Valeur B, Leray I (2000) Design principles of fluorescent molecular sensors for cation recognition. Coordination Chemistry Reviews 205 (1):3-40. doi:https://doi.org/10.1016/S0010-8545(00)00246-0

12. Berrocal MJ, Cruz A, Badr IH, Bachas LG (2000) Tripodal ionophore with sulfate recognition properties for anion-selective electrodes. Analytical chemistry 72 (21):5295-5299

13. Kang JH, Kim C (2018) Colorimetric detection of iron and fluorescence detection of zinc and cadmium by a chemosensor containing a bio-friendly octopamine. Photochemical & Photobiological Sciences 17 (4):442-452

14. Gupta VK, Singh AK, Kumawat LK, Mergu N (2016) An easily accessible switch-on optical chemosensor for the detection of noxious metal ions Ni (II), Zn (II), Fe (III) and UO_2 (II). Sensors and Actuators B: Chemical 222:468-482

15. Kim YS, Lee JJ, Lee SY, Jo TG, Kim C (2016) A highly sensitive benzimidazole-based chemosensor for the colorimetric detection of Fe (II) and Fe (III) and the fluorometric detection of Zn (II) in aqueous media. RSC advances 6 (66):61505-61515

16. Erdemir S, Kocyigit O (2016) Anthracene excimer-based "turn on" fluorescent sensor for Cr^{3+} and Fe^{3+} ions: Its application to living cells. Talanta 158:63-69

17. Schwarz FP, Wasik SP (1976) Fluorescence measurements of benzene, naphthalene, anthracene, pyrene, fluoranthene, and benzo [e] pyrene in water. Analytical chemistry 48 (3):524-528

18. Roek DP, Chateauneuf JE, Brennecke JF (2000) A fluorescence lifetime and integral equation study of the quenching of naphthalene fluorescence by bromoethane in super-and subcritical ethane. Industrial & engineering chemistry research 39 (8):3090-3096

19. Sahana A, Banerjee A, Das S, Lohar S, Karak D, Sarkar B, Mukhopadhyay SK, Mukherjee AK, Das D (2011) A naphthalene-based Al 3+ selective fluorescent sensor for living cell imaging. Organic & biomolecular chemistry 9 (15):5523-5529

20. Balabadra S, Kotni M, Manga V, Allanki AD, Prasad R, Sijwali PS (2017) Synthesis and evaluation of naphthyl bearing 1, 2, 3-triazole analogs as antiplasmodial agents, cytotoxicity and docking studies. Bioorganic & medicinal chemistry 25 (1):221-232

21. M. Shamsipur, M. Sadeghi, A. Garau, V. Lippolis (2013) An efficient and selective flourescent chemical sensor based on 5-(8-hydroxy-2-quinolinylmethyl)-2,8-dithia-5-aza-2,6-pyridinophane as a new fluoroionophore for determination of iron(III) ions. A novel probe for iron speciation, Analytica Chimica Acta 761:169-177

22. Fery-Forgues S, Lavabre D (1999) Are fluorescence quantum yields so tricky to measure: A demonstration using familiar stationery products. Journal of Chemical Education 76 (9):1260

23. Melhuish W (1961) Quantum efficiencies of fluorescence of organic substances: effect of solvent and concentration of the fluorescent solute1. The Journal of Physical Chemistry 65 (2):229-235

24. Tümay SO, Yeşilot S (2019) Tripodal synthetic receptors based on cyclotriphosphazene scaffold for highly selective and sensitive spectrofluorimetric determination of iron (III) in water samples. Journal of Photochemistry and Photobiology A: Chemistry 372:156-167

25. Hung H-C, Chi-Wen C, Ho I-T, Chung W-S (2009) Dual-mode recognition of transition metal ions by bis-triazoles chained pyrenes. Tetrahedron Letters 50:302–305

26. Hung H-C, Chi-Wen C, Wang Y-Y, Chen Y-J, Chung W-S (2009) Highly selective fluorescent sensors for Hg2+ and Ag+ based on bis-triazole-coupled polyoxyethylenes in MeOH solution. European Journal of Organic Chemistry: 6360–6366.

27. Çetindere S, Tümay SO, Kılıç A, Durmuş M, Yeşilot S (2016) Hexa-BODIPY linked-triazole based on a cyclotriphosphazene core as a highly selective and sensitive fluorescent sensor for Fe2+ ions. Journal of Fluorescence 26:1173–1181.

28. Senthilkumar T, Parekh N, Nikam SB, Asha S (2016) Orientation effect induced selective chelation of Fe^{2+} to a glutamic acid appended conjugated polymer for sensing and live cell imaging. Journal of Materials Chemistry B 4 (2):299-308

29. Zheng Y, Orbulescu J, Ji X, Andreopoulos FM, Pham SM, Leblanc RM (2003) Development of fluorescent film sensors for the detection of divalent copper. Journal of the American Chemical Society 125 (9):2680-2686

30. Pourreza N, Golmohammadi H (2015) Hemoglobin detection using curcumin nanoparticles as a colorimetric chemosensor. RSC Advances 5 (3):1712-1717

31. Morgounova E, Shao Q, Hackel BJ, Thomas DD, Ashkenazi S (2013) Photoacoustic lifetime contrast between methylene blue monomers and self-quenched dimers as a model for dual-labeled activatable probes. Journal of biomedical optics 18 (5):056004

32. Brummett AE, Schnicker NJ, Crider A, Todd JD, Dey M (2015) Biochemical, kinetic, and spectroscopic characterization of Ruegeria pomeroyi DddW—a mononuclear iron-dependent DMSP lyase. PloS one 10 (5)

33. Lakowicz JR (2013) Principles of fluorescence spectroscopy. Springer Science & Business Media

34. Cha K-W, Park K-W (1998) Determination of iron(III) with salicylic acid by the fluorescence quenching method. Talanta 46 (6):1567-1571. doi:https://doi.org/10.1016/S0039-9140(98)00032-0

35. S. Mirlohi, A.M. Dietrich, S.E. Duncan (2011) Age-associated variation in sensory perception of iron in drinking water and the potential for overexposure in the human population. Environmental Science & Technology 45(15):6575-6583

36. Andrade-Eiroa Á, Canle M, Cerdá V (2013) Environmental applications of excitation-emission spectrofluorimetry: an in-depth review I. Applied Spectroscopy Reviews 48 (1):1-49

37. Zhu X, Wang Z, Wu Z (2011) Characterization of membrane foulants in a full-scale membrane bioreactor for supermarket wastewater treatment. Process biochemistry 46 (4):1001-1009

38. Mobed JJ, Hemmingsen SL, Autry JL, McGown LB (1996) Fluorescence characterization of IHSS humic substances: total luminescence spectra with absorbance correction. Environmental science & technology 30 (10):3061-3065

Figure captions

Scheme 1. Synthetic pathway of compound **1**.

Fig 1. a) UV–Vis electronic absorption of 10 μM **1, b)** FL emission change of 2 μM **1**, **c)** naked-eye color changes and **d)** FL color changes of **1** in DMSO:water (1:1 v/v, pH 8.0 and λ_{ex}=345 nm) upon addition of 130 μM of various metal ions.

Fig 2. FL emission responses of 2 μM **1** in DMSO:water (1:1 v/v, pH 8.0 and λ_{ex}=345 nm) upon addition 130 μM of various competitive cations, anions and single molecules.

Fig 3. UV-vis **(a, b)** and FL titration **(c, d)** spectra of **1** with gradually increased amount of Fe^{3+} and F^- in DMSO:water (1:1 v/v, pH 8.0, λ_{ex}=345 nm and 10 μM of **1** for UV-Vis measurements, 2 μM of **1** for FL measurements).

Fig 4. Calibration curves of 2 μM **1** in DMSO:water (1:1 v/v, pH 8.0 and λ_{ex}=345 nm) for **a)** Fe^{3+} and **b)** F^-.

Fig 5. Excitation–emission matrix profile of **a) 1**, **b) 1** + Fe^{3+}, **c) 1** + Fe^{3+} + F^- in DMSO:water (1:1 v/v and pH 8.0).

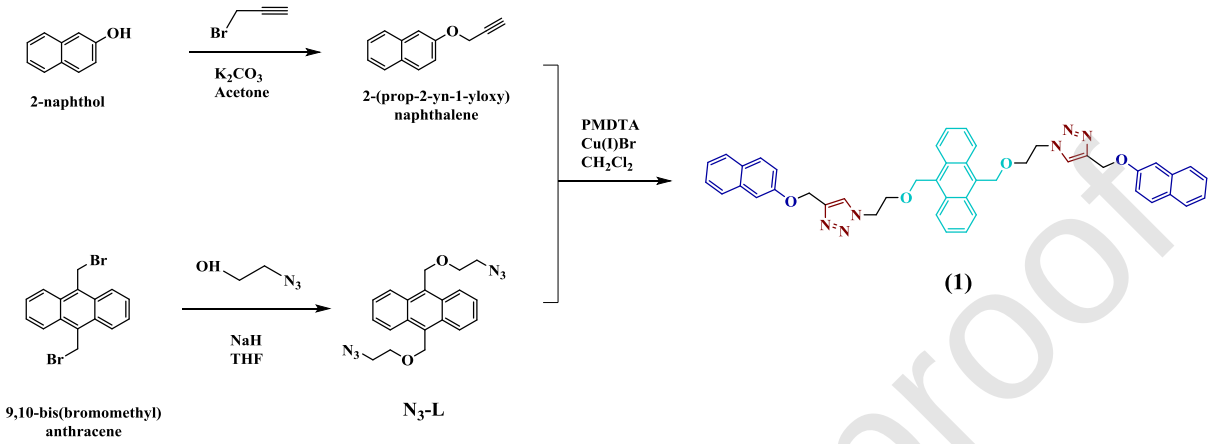

Scheme 1.

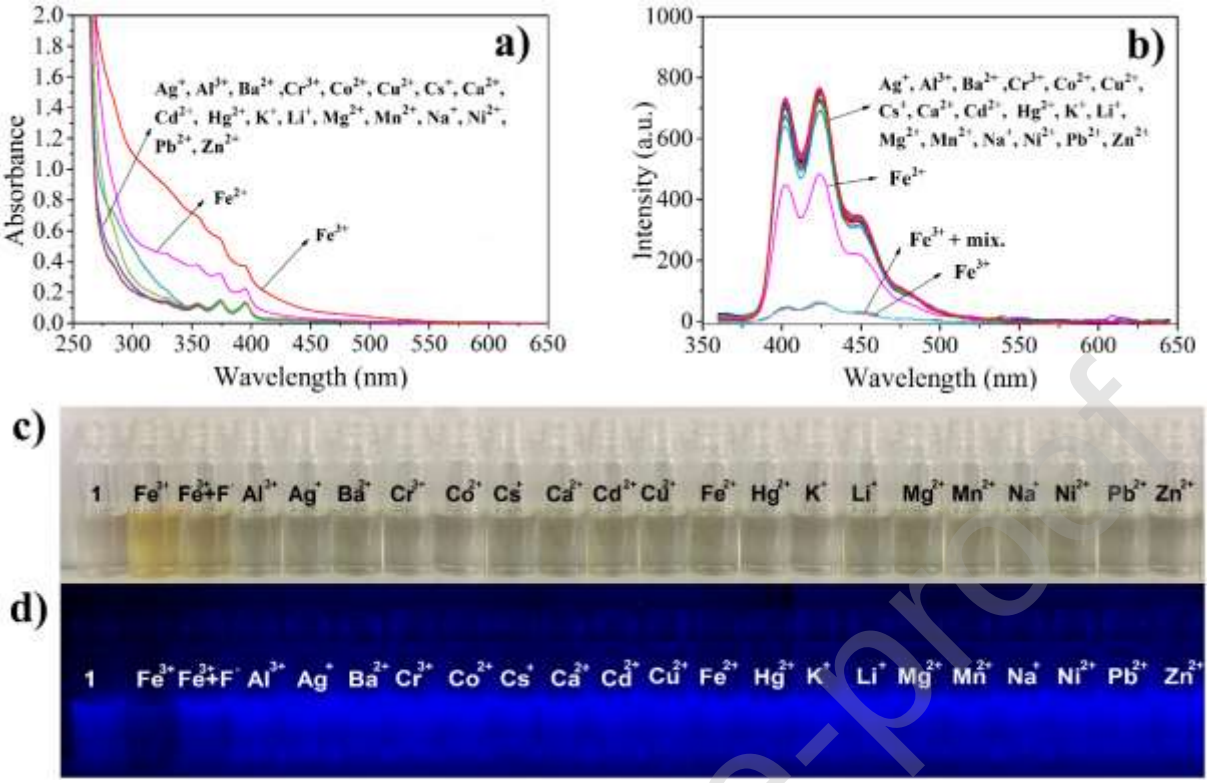

Fig 1.

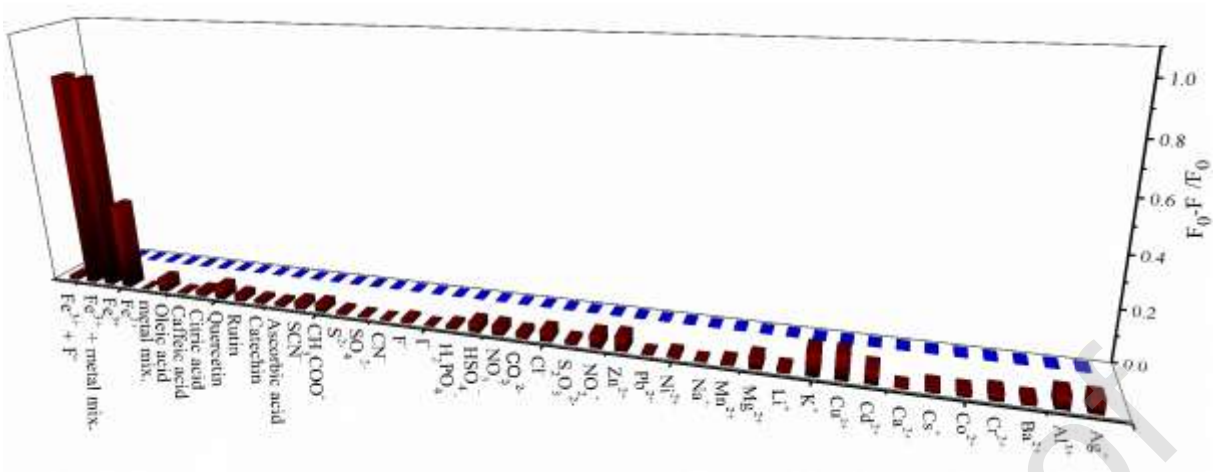

Fig 2.

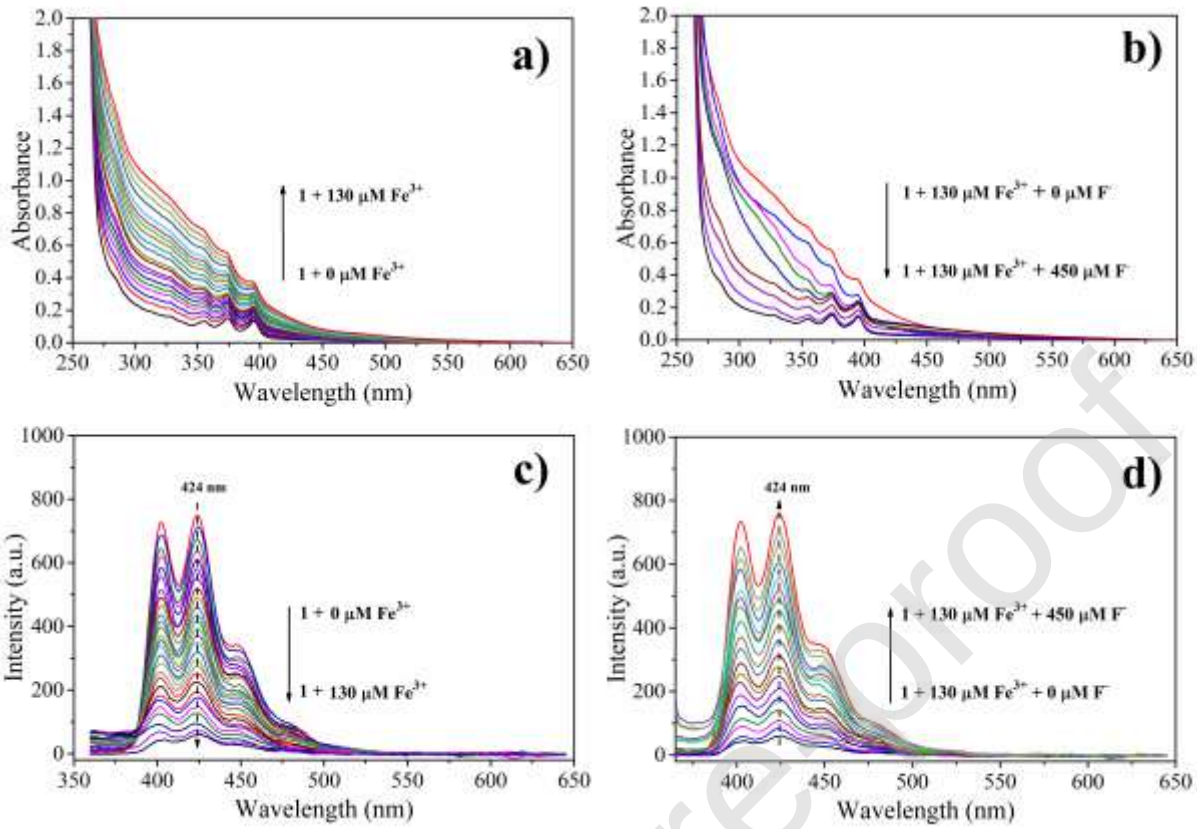

Fig 3.

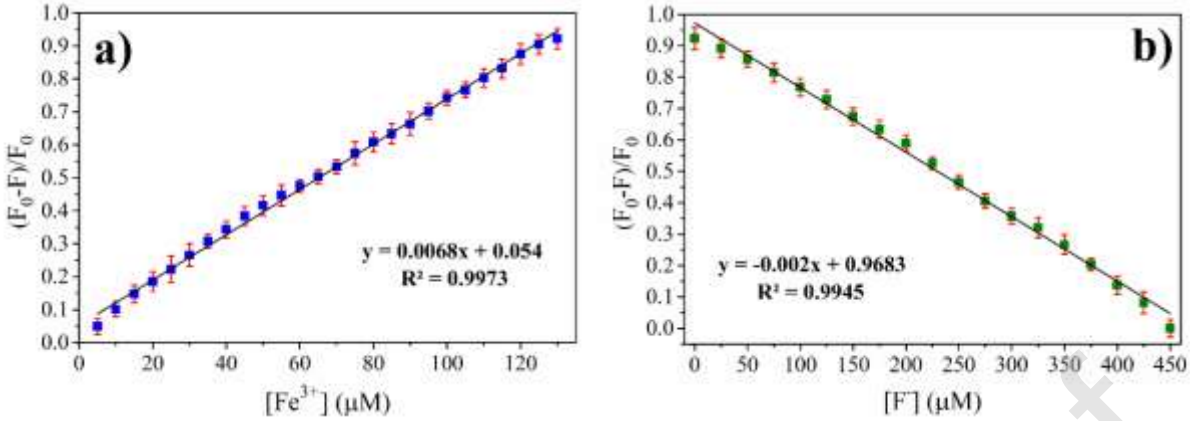

Fig 4.

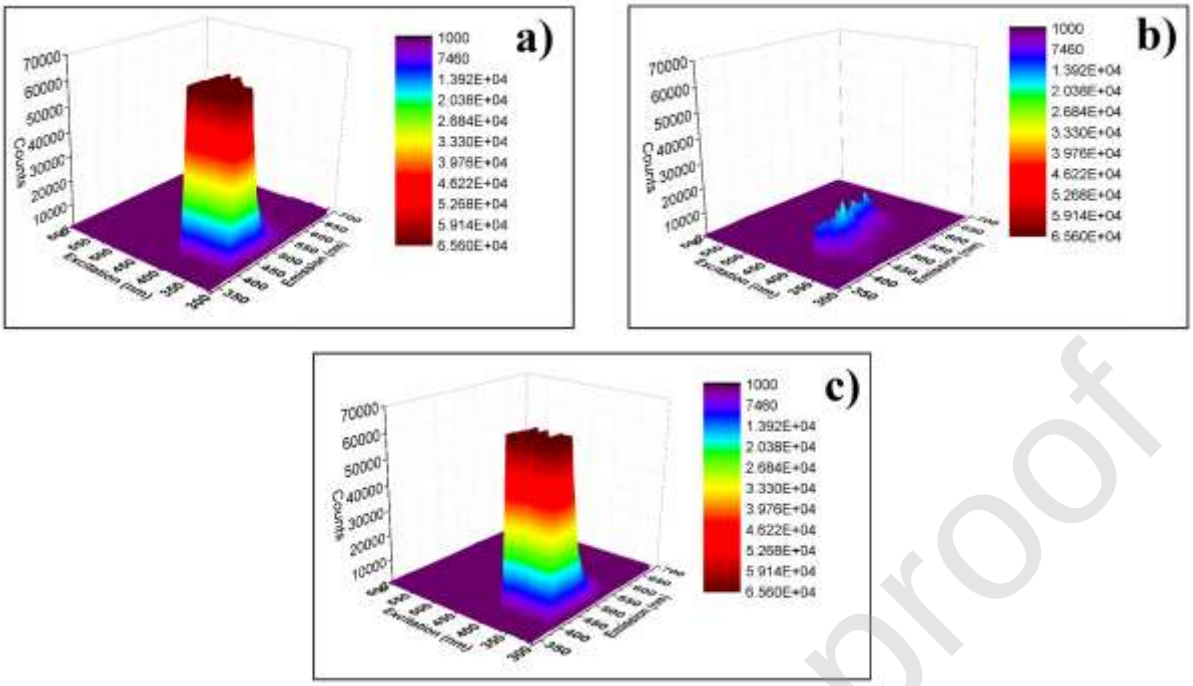

Fig 5.

Table 1. Spike and recovery tests of real samples.

Real Samples	Added (µM)	Detected (µM)	Recovery (%)
Sea Water	0	ND*	-
	50	49.03 ± 0.28	98.07
	75	76.14 ± 0.29	101.53
Tap Water	0	ND	-
	50	48.20 ± 0.15	96.39
	75	74.58 ± 0.54	99.44
Industrial Wastewater	0	56.39 ± 0.80	-
	50	108.06 ± 0.73	103.33
	75	133.22 ± 1.02	102.45
Tablet 1	0	36.47 ± 0.81	-
	50	84.85 ± 0.72	96.76
	75	114.86 ± 1.25	104.51
Tablet 2	0	30.75 ± 0.51	-
	50	82.02 ± 0.75	102.53
	75	107.08 ± 1.25	101.76
Tablet 3	0	32.68 ± 0.61	-
	50	83.37 ± 0.75	101.37
	75	106.10 ± 1.29	97.90

* Not detected

Table 2. Determination of iron in water samples and medicine tablet samples.

Proposed Method			ICP-OES	
Real Samples	**Found (ppm)**	**RSD (%)**	**Found (ppm)**	**RSD (%)**
Sea Water	BDL*	-	0.150 ± 0.0082	6.45
Tap Water	BDL	-	0.010 ± 0.0065	2.00
Industrial Wastewater	251.95 ± 2.95	1.17	249.50 ± 0.096	3.88
Tablet 1	162.94 ± 3.98	2.44	154.36 ± 0.8320	1.40
Tablet 2	137.39 ± 3.84	2.79	143.20 ± 0.1400	0.23
Tablet 3	146.01 ± 2.52	1.72	151.02 ± 0.7320	1.28

* Below detection limit